Rosenzweig–MacArthur Reaction–Diffusion Model

Ege Seçgin, Elia Salerno

January 18, 2026

Abstract

We investigate the spatial dynamics of the Rosenzweig-MacArthur predator-prey model using the Forward-Time Central-Space (FTCS) finite difference scheme on a 128×128 grid with periodic boundaries. Linear stability analysis reveals the coexistence equilibrium is locally an unstable node (trace $0.2333 > 0$, discriminant > 0), within the oscillatory Hopf bifurcation regime driven by the "paradox of enrichment". Differential diffusion ($D_u/D_v = 10$) amplifies oscillations into periodic traveling waves and spatiotemporal chaos, distinct from static Turing patterns which typically require the "fear effect". High prey diffusion conversely promotes spatial synchronization.

1 Declaration of AI Usage

The LLM's "Gemini Flash 2.5 and 3" from Google and "ChatGPT 5.1" from OpenAI were used to assist in ideation for exploration and to formalize the written style of this report. The report itself and the accompanying code are our own work, all LLM output has been verified with evidence from literature[1, 2, 3, 4]. We found the LLM's unreliable for sourcing but helpful for simplifying mathematical concepts based on literature and improving text conciseness.

2 The Mathematical Model

2.1 Model Description

The Rosenzweig–MacArthur model [1] extends the Lotka-Volterra system with logistic prey growth and Holling type-II functional response. Adding spatial diffusion enables analysis of pattern formation and traveling waves not seen in non-spatial models. Unlike ratio-dependent models or those including the "fear effect" which can support static Turing patterns, this standard formulation typically yields dynamic instabilities like spatiotemporal chaos or traveling waves in the oscillatory regime [3, 5, 6].

2.2 Governing Equations

The system describes the spatiotemporal evolution of prey density $u(x, y, t)$ and predator density $v(x, y, t)$:

$$\frac{\partial u}{\partial t} = D_u \nabla^2 u + ru\left(1 - \frac{u}{K}\right) - \frac{\alpha uv}{1 + hu} \tag{1}$$

$$\frac{\partial v}{\partial t} = D_v \nabla^2 v + \beta \frac{\alpha uv}{1 + hu} - mv \tag{2}$$

where ∇^2 denotes the Laplacian operator in two spatial dimensions.

2.3 Parameters and Values

The baseline simulation uses the diffusion ratio $D_u/D_v = 10$ to ensure fast prey dispersal relative to predators. All values are selected within the typical ranges provided in the assignment prompt, so the

interpretation in physical units is preserved.

- u, v: Densities (ind/m^2)
- $D_u = 0.5$: Prey Diff. (m^2/d)
- $D_v = 0.05$: Pred. Diff. (m^2/d)
- $r = 0.5$: Growth rate (d^{-1})
- $K = 500.0$: Carrying capacity
- $\alpha = 0.01$: Attack rate
- $h = 0.05$: Handling time
- $\beta = 0.3$: Conversion eff.
- $m = 0.05$: Mortality rate

2.4 Numerical Implementation

We use the FTCS finite difference scheme on a 128×128 grid ($L = 100$ m, $\Delta x \approx 0.78$ m) with periodic boundaries. The Laplacian uses a five-point stencil and time integration uses forward Euler:

$$u_{i,j}^{n+1} = u_{i,j}^n + \Delta t \left[D_u \frac{u_{i+1,j}^n + u_{i-1,j}^n + u_{i,j+1}^n + u_{i,j-1}^n - 4u_{i,j}^n}{(\Delta x)^2} + R_u(u_{i,j}^n, v_{i,j}^n) \right] \tag{3}$$

where R_u is the reaction term. Negative densities are set to zero. The method is first-order in time ($O(\Delta t)$) and second-order in space ($O(\Delta x^2)$).

3 Stability Analysis

3.1 Coexistence Equilibrium

Setting the reaction terms in (1)–(2) to zero yields the homogeneous coexistence equilibrium

$$u^* = \frac{m}{\beta\alpha - mh}, \qquad v^* = \frac{r}{\alpha}(1 + hu^*)\left(1 - \frac{u^*}{K}\right), \tag{4}$$

which exists for $\beta\alpha > mh$ and $0 < u^* < K$. For the baseline parameters, $u^* = 100.0$ and $v^* = 240.0$.

3.2 Numerical Stability

The CFL condition for 2D diffusion requires $\Delta t \leq (\Delta x)^2/(4\max(D_u, D_v))$, yielding $\Delta t_{\max} \approx 0.305$ d. To account for reaction stiffness, we use

$$\Delta t = \min\left(0.9\,\Delta t_{\max},\ 0.1\left(\max(r, m, \alpha)\right)^{-1}\right) = 0.2 \text{ d}, \tag{5}$$

and enforce non-negativity after each update.

3.3 Linear Stability Analysis

The Jacobian of the reaction terms at (u^*, v^*) yields:

$$\text{trace}(J) = 0.2333 > 0, \quad \det(J) = 0.0033 > 0 \tag{6}$$

The positive discriminant ($\Delta \approx 0.0412 > 0$) confirms the eigenvalues are real and positive, characterizing the equilibrium locally as an unstable node. Trajectories are repelled monotonically from the equilibrium before settling into a global limit cycle. This oscillatory instability is driven by the "paradox of enrichment," where increasing K destabilizes the steady state. Since the trace is positive, the system operates outside the standard Turing regime (which requires stable local kinetics), leading to dynamic spatiotemporal patterns rather than static structures.

4 Results and Discussion

4.1 Simulation Design

Two numerical experiments were run: (i) a baseline simulation ($D_u/D_v = 10$) for $t \in [0, 500]$ d with two localized circular perturbations to trigger wave emergence, and (ii) a diffusion-ratio comparison for $t = 300$ d using a single central perturbation and three diffusion regimes. The purpose is to connect stability properties to emergent spatial patterns.

4.2 Temporal Evolution

Figure 1 shows evolution from localized perturbations in the baseline regime. By $t = 50$ d, perturbations expand into concentric waves. By $t = 200$ d, the wavefronts interact to form quasi-periodic structures, and at $t = 400$ d, a stable pattern of periodic traveling waves persists, confirming the oscillatory nature of the instability.

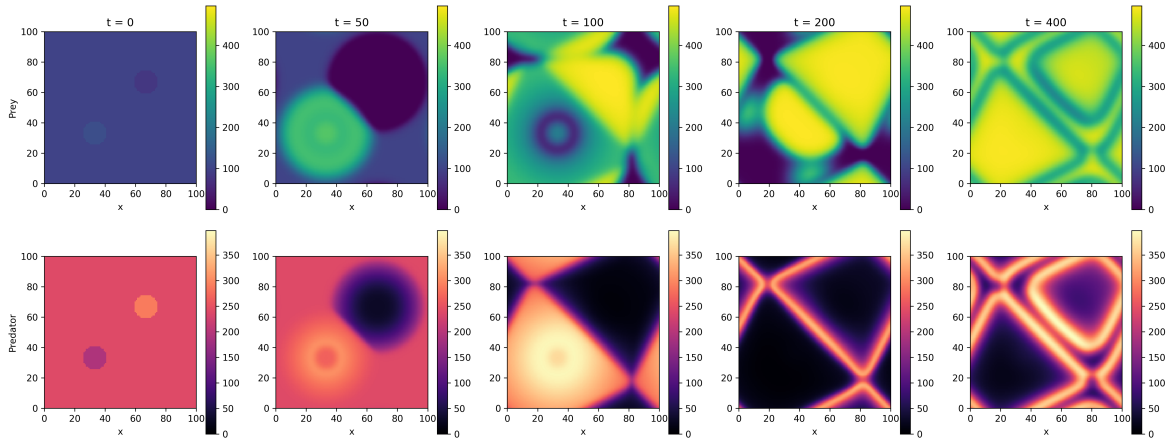

Figure 1: Temporal evolution of prey (top) and predator (bottom) densities at $t = 0, 50, 100, 200, 400$ d. Initial perturbations spread as periodic traveling waves, evolving into complex spatiotemporal patterns.

At $t = 500$ d (Figure 2), high prey regions correspond to low predator density with a phase lag reflecting predation time delays. The predator density peaks at the wavefronts of the prey expansion, creating a chasing dynamic.

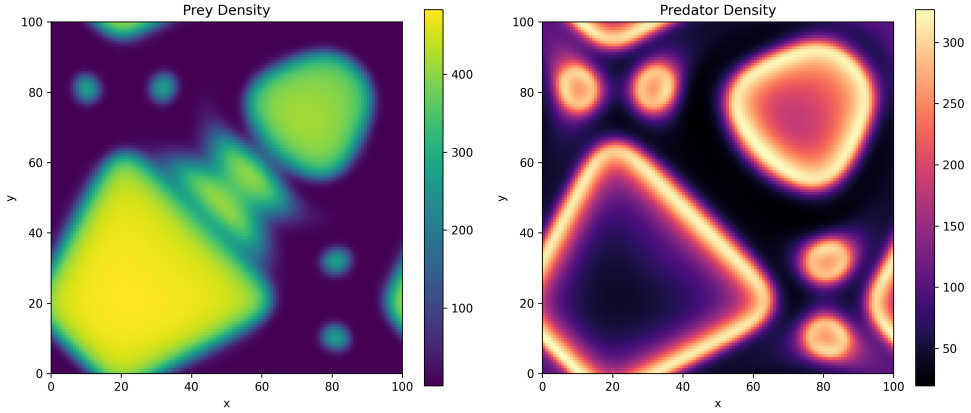

Figure 2: Final spatial distributions at $t = 500$ d. Prey density (left) and predator density (right) show strong spatial inverse correlation, driven by the predation phase lag.

4.3 Diffusion Ratio Analysis

Figure 3 compares three regimes at $t = 300$ d. The results demonstrate how diffusion rates modulate the coupling of local oscillators.

Fast Prey Diffusion ($D_u/D_v = 5$) leads to spatial synchronization. The rapid dispersal of prey suppresses spatial gradients, causing the domain to oscillate largely in phase (global limit cycle) rather than forming localized structures. Initial numerical indications of predator extinction were identified as artifacts; the analytical predator per-capita growth rate at prey carrying capacity is positive (≈ 0.0077 d^{-1}), ensuring predator survival even if densities remain low during transient phases.

Fast Predator Diffusion ($D_u/D_v = 0.2$) generates high-contrast spatiotemporal chaos. The high predator mobility prevents phase locking, resulting in sharp wavefronts and significant density variations, consistent with findings on chaos in excitable media where the predator "outruns" the prey expansion.

Equal Diffusion ($D_u/D_v = 1$) results in broad, domain-filling traveling waves. The matched diffusion rates facilitate the propagation of the instability across the grid without the homogenizing effect of fast prey diffusion, maintaining high prey densities ($u \in [100, 400]$) across the majority of the domain.

5 Conclusions

We analyzed the Rosenzweig–MacArthur reaction–diffusion model using an FTCS scheme. The coexistence equilibrium is locally an unstable node, driving global limit cycles via the paradox of enrichment. Differential diffusion strongly influences the spatial morphology: fast predator diffusion ($D_v > D_u$) yields the sharpest, high-contrast patterns through phase-decoupling, whereas fast prey diffusion ($D_u > D_v$) promotes spatial synchronization and homogenization. These results highlight that in oscillatory excitable media, the ratio of diffusion coefficients dictates the coupling and synchronization of local populations rather than creating static Turing structures.

References

[1] M. L. Rosenzweig and R. H. MacArthur. Graphical Representation and Stability Conditions of Predator-Prey Interactions. *The American Naturalist*, 97(895):209–223, July 1963.

[2] Katrin Grunert, Helge Holden, Espen R. Jakobsen, and Nils Chr. Stenseth. Evolutionarily stable strategies in stable and periodically fluctuating populations: The Rosenzweig–MacArthur predator–prey model. *Proceedings of the National Academy of Sciences*, 118(4):e2017463118, January 2021.

[3] R. Stephen Cantrell and Chris Cosner. *Spatial Ecology via Reaction-Diffusion Equations*. Wiley, Hoboken, NJ, 2003.

[4] Michael Begon and Colin R. Townsend. *Ecology: From Individuals to Ecosystems*. Wiley, Hoboken, NJ, 2021.

[5] Weiming Wang, Quan-Xing Liu, and Zhen Jin. Spatiotemporal complexity of a ratio-dependent predator-prey system. *Physical Review E*, 75(5):051913, May 2007.

[6] Martin Baurmann, Thilo Gross, and Ulrike Feudel. Instabilities in spatially extended predator–prey systems: Spatio-temporal patterns in the neighborhood of Turing–Hopf bifurcations. *Journal of Theoretical Biology*, 245(2):220–229, March 2007.

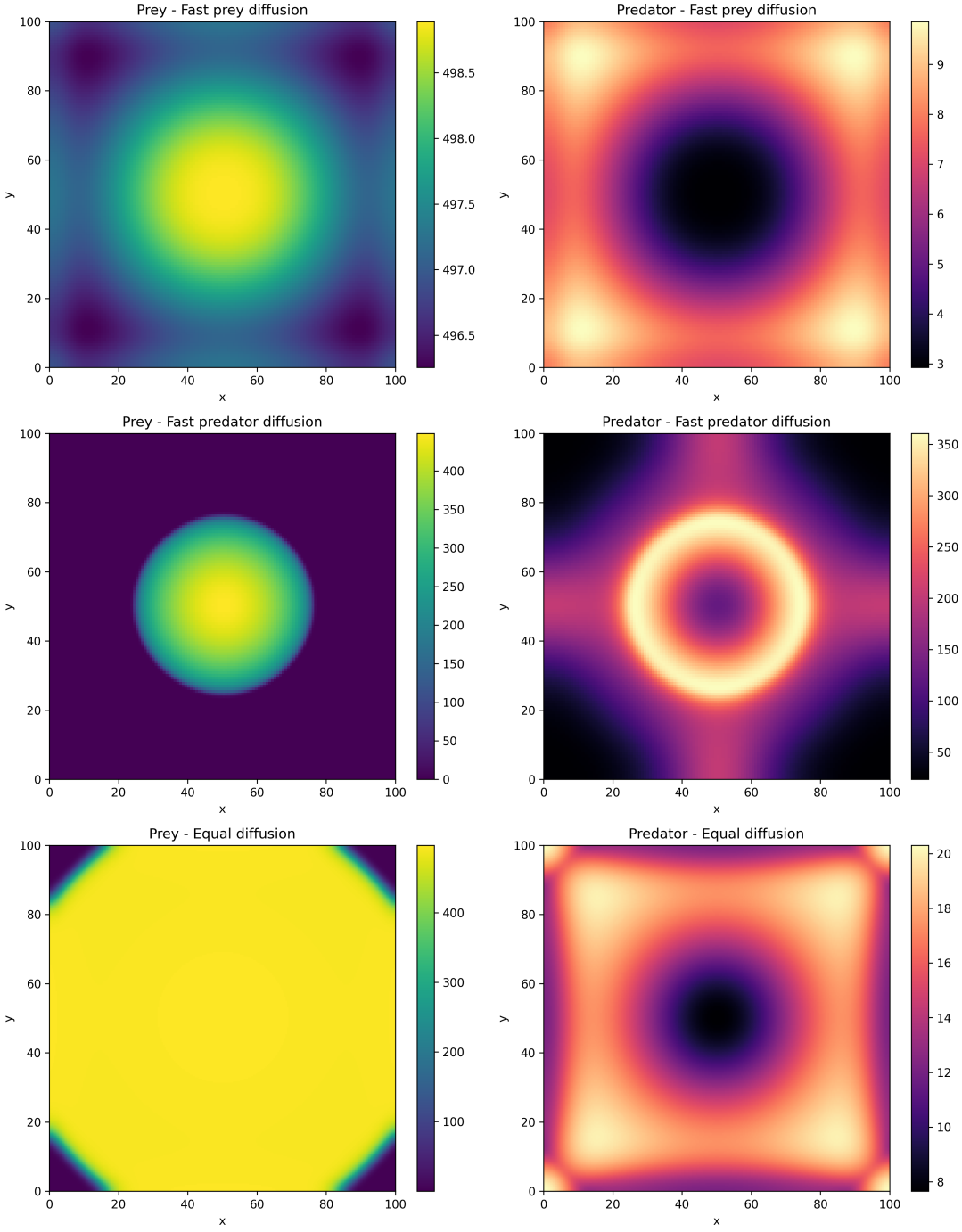

Figure 3: Comparison of diffusion regimes at $t = 300$ d. Top: Fast prey diffusion ($D_u/D_v = 5$) results in near-homogenization of prey at carrying capacity ($u \approx 498$) with minimal spatial variation and low predator densities ($v < 10$). Middle: Fast predator diffusion ($D_u/D_v = 0.2$) maintains sharp, high-amplitude spatial structures with significant density ranges for both species. Bottom: Equal diffusion ($D_u/D_v = 1$) exhibits a domain-filling expansion of prey with high density, while predator densities remain comparatively low ($v \in [8, 20]$).